LENTIVIRAL-BASED REPORTER CONSTRUCTS FOR PROFILING CHONDROGENIC ACTIVITY IN PRIMARY EQUINE CELL POPULATIONS

A. Martin-Pena[1], R.M. Porter[2], G. Plumton[3], T.M. McCarrel[4], A.J. Morton[4], M.V. Guijarro[5],
S.C. Ghivizzani[1], B. Sharma[2] and G.D. Palmer[1,*]

[1] Department of Orthopaedics and Rehabilitation, University of Florida, Gainesville, FL, USA
[2] Department of Orthopaedics, University of Arkansas, Little Rock, AR, USA
[3] Department of Biomedical Engineering, University of Florida, Gainesville, FL, USA
[4] College of Veterinary Sciences, University of Florida, Gainesville, FL, USA
[5] Department of Anatomy and Cell Biology, University of Florida, Gainesville, FL, USA

Abstract

Successful clinical translation of mesenchymal stem cell (MSC)-based therapies for cartilage repair will likely require the implementation of standardised protocols and broadly applicable tools to facilitate the comparisons among cell types and chondroinduction methods. The present study investigated the utility of recombinant lentiviral reporter vectors as reliable tools for comparing chondrogenic potential among primary cell populations and distinguishing cellular-level variations of chondrogenic activity in widely used three-dimensional (3D) culture systems. Primary equine MSCs and chondrocytes were transduced with vectors containing combinations of fluorescent and luciferase reporter genes under constitutive cytomeglavirus (CMV) or chondrocyte-lineage (Col2) promoters. Reporter activity was measured by fluorescence imaging and luciferase assay. In 3D cultures of MSC aggregates and polyethylene glycol-hyaluronic acid (PEG-HA) hydrogels, transforming growth factor beta 3 (TGF-β3)-mediated chondroinduction increased Col2 reporter activity, demonstrating close correlation with histology and mRNA expression levels of *COL2A1* and *SOX9*. Comparison of chondrogenic activities among MSC populations using a secretable luciferase reporter revealed enhanced chondrogenesis in bone-marrow-derived MSCs relative to MSC populations from synovium and adipose tissues. A dual fluorescence reporter – enabling discrimination of highly chondrogenic (Col2-GFP) cells within an MSC population (CMV-tdTomato) – revealed marked heterogeneity in differentiating aggregate cultures and identified chondrogenic cells in chondrocyte-seeded PEG-HA hydrogels after 6 weeks in a subcutaneous implant model – indicating stable, long-term reporter expression *in vivo*. These results suggested that lentiviral reporter vectors may be used to address fundamental questions regarding chondrogenic activity in chondroprogenitor cell populations and accelerate clinical translation of cell-based cartilage repair strategies.

Introduction

For over two decades, adult mesenchymal stem/progenitor cells (MSCs) have been regarded as highly preferable cell type for autologous cell-based cartilage repair (Matsumoto e*t al.*, 2010; Roelofs *et al.*, 2013). Their prevalence in many tissues, high expansion potential and accessibility overcome many of the problems associated with the use of articular chondrocytes, including limited availability, donor site morbidity and phenotypic instability (Jayasuriya *et al.*, 2015; Matricali *et al.*, 2010). However, the clinical advancement of MSC and other cell-based therapies for cartilage repair is hindered by the wide variation in pre-clinical models used among laboratories and associated differences in cell culture, differentiation

protocols and implantation strategies (Goldberg *et al.*, 2017). As a result, despite numerous reports of improved healing in animal studies (Bornes *et al.*, 2014; Goldberg *et al.*, 2017; Huang *et al.*, 2017; Lo Monaco *et al.*, 2018), there is still no consensus regarding the efficacy of the used strategies and a clear pathway to clinical translation has yet to emerge. Within the MSC field, this disparity is exacerbated by the poor characterisation of primary cell populations and the lack of standardised tools for quantifying chondrogenic potential and cartilage repair. In particular, using current techniques, it is difficult to determine if MSCs uniformly undergo chondrogenesis or directly participate in neocartilage formation *in vivo*.

A consensus regarding which autologous cell sources, chondrocytes or various MSC subtypes, are most useful for cartilage repair has yet to be established. MSCs from bone marrow (Johnstone *et al.*, 1998; Mackay *et al.*, 1998), fat (Khan *et al.*, 2012; Nathan *et al.*, 2003; Veronesi *et al.*, 2013; Wickham *et al.*, 2003) and synovium (Pei *et al.*, 2008; Sakaguchi *et al.*, 2005; Shirasawa *et al.*, 2006) are widely investigated and purportedly enhanced chondrogenic activity is reported for synovial-derived MSCs (Sakaguchi *et al.*, 2005; Yoshimura *et al.*, 2007) and cartilage-derived stem cells (McCarthy *et al.*, 2012; Williams *et al.*, 2010). However, the lack of universally adopted methods for assessing chondrogenic potential prevents meaningful study-to-study comparisons. Histology-based assessments of MSC chondrogenesis *in vitro* and *in vivo* are essential for visualising cartilage ECM components and the nature of chondrocyte differentiation but provide limited sensitivity for meaningful quantitative comparisons of chondrogenesis among different cell preparations (Orth *et al.*, 2015). On the other hand, biochemical and molecular measurement of chondrocyte markers or ECM synthesis offer quantitative measures but often require pooling of samples and do not distinguish cellular-level responses (McLeod *et al.*, 2017).

Transcriptional reporter systems comprised of fluorescent or bioluminescent cDNAs under regulatory control of promoters or response elements of chondrocyte marker genes, including *ACAN* (Hung *et al.*, 2000; Palmer *et al.*, 2001) *COL11A2* (Outani *et al.*, 2013) and *COL2A1* (Kan *et al.*, 2009; Padmashali *et al.*, 2014; Porter *et al.*, 2012; Stokes *et al.*, 2001), are used as quantitative indicators of chondrocyte activity in cell culture and transgenic models. However, their application as tools to monitor cartilage differentiation and repair in cell and tissue engineering protocols has not been explored. In the present study, the utility of lentiviral-vector-based transcriptional reporter constructs that incorporate a modified collagen type 2 (Col2) promoter was explored for the evaluation of chondrogenesis of post-natal, primary equine MSCs and chondrocytes. The vectors, containing bicistronic or independent expression cassettes encoding combinations of fluorescence and luciferase-based reporters, were used to demonstrate chondrocyte-specific activity and evaluate chondrogenic potential within and among primary cell populations. Reporter activity was measured by fluorescence imaging, flow cytometry or luciferase assay in widely used cell aggregate and hydrogel culture models of chondrogenesis and validated by conventional assessments of chondrogenic differentiation. The utility of these reporters for assessment of cell fate after *in vivo* implantation was also evaluated.

Materials and Methods

Generation of recombinant lentiviral reporter vectors

Bicistronic lentiviral vector- Lv.Col2-GFP/fLuc
A promoter sequence was synthesised based on a previous design (Kan *et al.*, 2009): four repeats of a highly conserved enhancer region within the first intron of *COL2A1* (+ 2126/+ 2174 bp), which contains a *SOX9* binding motif (Zhou *et al.*, 1998), were positioned upstream of the core *COL2A1* promoter (− 164/+ 37 bp). These regulatory sequences were flanked by the restriction sites for SpeI (5' end) and BamHI (3' end) and an NheI site was placed between the four enhancer repeats and the core *COL2A1* promoter. This promoter was synthesised by GenScript (Piscataway, NJ, USA) and cloned in place of a truncated, "minimal" cytomegalovirus (mCMV) promoter within the third-generation lentiviral expression plasmid pTRH1-mCMV-dscGFP-T2A-Fluc (System Biosciences, Mountain View, CA, USA). In the resulting reporter construct, pGF-4eCOL2A1 (Addgene ID# 97210; Addgene, Cambridge, MA, USA), the promoter drives the co-expression of copepod green fluorescent protein (copGFP) and firefly luciferase using the *Thosea asigna* virus 2A (T2A) self-cleaving peptide (Kim *et al.*, 2011). Replication-deficient lentivirus was generated by transfecting 293T cells with pGF-4eCOL2A1 and the third-generation packaging plasmids pMDLg/pRRE (Addgene ID# 12251), pRSV-Rev (Addgene ID# 12253) and pMD2.G (Addgene ID# 12259) (Dull *et al.*, 1998).

Dual promoter reporter vectors – Lv.CMV-mLuc/EF1-GFP, Lv.Col2-mLuc/EF1-GFP and Lv.CMV-tom/Col2-GFP
For generation of dual lentiviral reporter vectors with independent expression cassettes under separate regulation of constitutive (CMV or EF1α) and chondrogenic (Col2) promoters, the pcDH lentiviral expression system (System Biosciences) was used. A modified pcDH lentiviral expression plasmid, pcDH-CMV-mLuc/EF1-GFP, containing independent CMV-mLuc and EF1-GFP expression cassettes was generated by cloning the full-length cDNA of *Metridia* luciferase (mLuc) from the pMetLuc reporter vector (Takara Bio, Mountain View, CA; USA) into the multiple cloning site of pcDH-CMV-MCS-EF1-copGFP using compatible

Table1. Primers sequences to generate a pcDH-CMV-tom/Col2-GFP lentiviral expression plasmid.

Primer sequence	Orientation
5'-TTATCGAT<u>GCGGCCGCG</u>AACTAGTCTGTGAATCG-3'	forward
5'-CGCATGTTA<u>GTCGAC</u>TTCCTCTGCCCTCACCG-3'	reverse

BamHI/NotI restriction sites. To generate a lentiviral expression plasmid with mLuc under control of a Col2 promoter, pcDH-Col2-mLuc/EF1-GFP, the CMV promoter sequence was removed from pcDH-CMV-mLuc/EF1-GFP and replaced with the Col2 promoter sequence from pGF-4eCOL2A1 using compatible SpeI/BamHI restriction sites. For generation of a dual fluorescence reporter containing independent CMV-tom and Col2-GFP expression cassettes, the full-length cDNA of tdTomato was obtained by BamHI/NotI digestion of pCSCMV:tdTomato (Addgene ID# 30530) and cloned into the multiple cloning site of pcDH to generate pcDH-CMV-tom/EF1-GFP. Then, the EF1-GFP cassette was replaced with a Col2-GFP expression cassette flanked by NotI (5' end; underlined in the primer sequence) and SalI (3' end; underlined in the primer sequence) restriction sites, introduced by PCR amplification of pGF-4eCOL2A1 using the primers listed in Table 1, to generate a pcDH-CMV-tom/Col2-GFP lentiviral expression plasmid. For production of replication-deficient lentiviral vectors, each pcDH lentiviral expression plasmid was transfected into 293T cells with the second generation packaging plasmids pSPAX-2 (Addgene ID# 12260) and pMD2.G. Viral supernatants were harvested 48 h after transfection and either used directly for cell transduction or concentrated to 1/50th of the initial volume using the Lenti-X concentrator reagent and protocol (Takara).

Viral-titering

Quantitation of lentiviral vectors from culture supernatants or concentrated virus was performed using the QuickTiter™ Lentivirus Titer Kit (Cell Biolabs, San Diego, CA, USA). Physical titers were determined based on the detection of lentivirus-associated HIV p24 and ranged from 2.5×10^9-2×10^{10} vp/mL.

Cell and tissue harvest

Cartilage, bone-marrow, synovium and adipose tissues were collected from horses (age range: 2-12 years) euthanised for health issues unrelated to musculoskeletal conditions at the UF School of Veterinary Medicine, Gainesville, FL, USA.

Articular chondrocytes

Intact, healthy cartilage was obtained from the femoropatellar, metacarpophalangeal and scapulohumeral joints, minced finely and digested with 0.2 % collagenase type II (Worthington, Biochemical Corporation, Lakewood, NJ, USA) for 12-16 h at 37 °C, 5 % CO_2 in DMEM/F12 (ThermoFisher Scientific) supplemented with 5 % foetal bovine serum (FBS) (Hyclone Laboratories, South Logan, UT, USA). Cell suspensions were filtered through a 70 μm strainer and plated at density of 50,000 cells/cm^2 in high glucose Dulbecco's modified Eagle medium (DMEM) (Corning) supplemented with 10 % FBS. Within 3 d of harvest, primary chondrocytes were replated at 80 % confluence until required.

Synoviocytes

The non-collagenous soft tissues, including the synovial lining and subsynovium, were scraped from the capsular tissues of the carpal joints, minced and digested in saline solution with 0.2 % collagenase for 2 h at 37 °C and 5 % CO_2, as previously described (Watson *et al.*, 2013). Non-adherent cells were removed after 24 h and, after 1 week, cells were replated at high density until required.

Bone-marrow-derived MSCs

Bone marrow aspirate (~ 15 mL) was obtained by needle puncture of the iliac crest, mixed 1 : 1 with MSC isolation medium [low glucose DMEM with 20 % FBS and 10 ng/mL fibroblast growth factor 2 (FGF-2) (Peprotech)] and plated at 500,000 nucleated cells/cm^2. After 3 d, the media was replaced with MSC expansion medium (low glucose DMEM supplemented with 10 % FBS and 10 ng/mL FGF-2) and the cells were cultured until reaching confluency (~ 10 d).

Synovial-derived MSCs

~ 2-3 g of synovial tissue were harvested from the intercarpal and femoropatellar joints and digested with 0.1 % trypsin in phosphate buffered saline (PBS) for 30 min followed by treatment for 2 h at 37 °C and 5 % CO_2 with 0.1 % collagenase in serum-free high glucose DMEM, as previously described (He *et al.*, 2009). After digestion, cells were filtered through a 45 μm strainer and plated until confluency was reached (~ 7 d).

Adipose-derived MSCs

~ 8-10 g of adipose tissue were harvested from the subcutaneous fat depot lateral to the tail head. The tissue was diced into small pieces and digested for 3 h at 37 °C, 5 % CO_2 with 0.2 % collagenase in serum-free DMEM. After digestion, cells were filtered through a 45 μm strainer and plated until confluency (~ 7 d). After initial plating in T-75 flasks (P0), all MSC populations were expanded at 5,000 cells/cm^2 in MSC expansion medium until required.

To verify the colony-forming potential of MSC populations, primary cell isolates were plated into 6-well plates and cultured in MSC expansion

medium. After 10 d, colonies were fixed with 10 % neutral buffered formalin (NBF) for 15 min and stained with 1 % crystal violet for 1 h at room temperature. Colony numbers per 10^3 nucleated cells were as follows: 0.02 ± 0.002 BM-MSCs; 12 ± 3.2 S-MSCs; 2.9 ± 1.8 A-MSCs.

Lentiviral transduction

Primary cells (passage 2-4) were seeded into 6-well plates and the culture media replaced with 1 mL/well serum-free DMEM containing 8 μg/mL polybrene (Sigma-Aldrich) and 293T viral supernatants or concentrated virus. For transduction, cells were infected (dose range: 1.3×10^3-6.4×10^3 vp/cell) by centrifugation at 1,200 ×*g* for 60 min, followed by an additional 2 h in a tissue culture incubator at 37 °C, 5 % CO_2. Then, the virus-containing medium was removed and replaced with growth medium and cells were replated into T-150 flasks until required. Transduction efficiencies, determined by tdTomato or GFP flow cytometry, were ~ 70 % or higher for all viral vectors and cell types used in the study. At the vector doses used, impaired chondrogenic activity of equine MSCs were not observed (data not shown).

In vitro chondrogenesis

Aggregate culture

Lentiviral-reporter-labelled MSCs and chondrocytes were trypsinised from monolayer cultures and seeded at 5×10^5 cells/mL in 15 mL polypropylene tubes, centrifuged at 500 ×*g* for 5 min to induce aggregate formation and maintained in 0.5 mL of chondrogenic medium consisting of serum-free, high glucose DMEM containing pyruvate (1 mM), 1 % ITS™ Premix (BD Biosciences), 37.5 μg/mL ascorbate 2-phosphate and 10^{-7} M dexamethasone (Johnstone *et al.*, 1998). To induce chondrogenesis, media was supplemented with 10 ng/mL human transforming growth factor beta 3 (TGF-β3; Peprotech).

Photopolymerisable PEG-HA hydrogels

Labelled cells (2×10^7 cells/mL) were mixed with a polymer solution of 10 % w/v PEODA (Laysan Bio, Arab, AL, USA), 0.05 % w/v Irgacure 2959 photoinitiator (Sigma-Aldrich) and 2.5 mg/mL hyaluronic acid (1,100 kDa; Lifecore Biomedical) in sterile PBS (Sharma *et al.*, 2007). Next, the cell-polymer solution was pipetted into plastic moulds and placed under a long-wave, 365 nm ultraviolet light at 4 mW/cm^2 (Omincure S2000, Excelitas Technologies, Mississauga, ON, Canada) for 5 min to induce polymerisation and generate 5 × 3 mm cylindrical constructs. Then, the constructs were transferred into 24-well plates filled with chondrogenic medium for *in vitro* studies or implantation experiments.

Subcutaneous implantation

All procedures involving animals were conducted according to protocols approved by the University of Florida Institutional Animal Care and Use Committee. For surgery, athymic nude mice (Charles River) were anaesthetised by isofluorane inhalation and prepped for surgery following sedation. Under aseptic conditions, subcutaneous pockets were made by generating two 10 mm-long dorsal midline incisions and gently spreading the cutaneous tissue lateral to each incision line creating a total of 4 pockets per animal. Then, sterile cell-seeded polyethylene glycol-hyaluronic acid (PEG-HA) scaffolds, approximately 5 mm in diameter, 3 mm-thick, were securely implanted into each pocket away from the incision area. Following wound closure using wound clips, the animals were removed from anaesthesia and returned to free cage activity for the duration of the experiments.

Flow cytometry and cell sorting

For assessment of transfection efficiency of Lv.Col2-GFP/fLuc and Lv.CMV-GFP/fLuc vectors, monolayer cultures were trypsinised, washed in PBS and resuspended in PBS/0.05 % bovine serum albumin (BSA) at 5×10^6 cells/mL. GFP fluorescence was analysed using an LSRII flow cytometer (BD BioSciences). For sorting of GFP+/tdTomato+ and GFP−/tdTomato+ subpopulations in differentiating BM-MSC aggregates by fluorescence-activated cell sorting (FACS), Lv.CMV-tom/Col2-GFP-transduced aggregates were pooled (*n* = 7-8) and digested with a mixture of 0.1 % collagenase and Tryple Select Enzyme (ThermoFisher Scientific) for 45 min at 37 °C. Recovered cells were resuspended in sterile PBS/0.05 % BSA at 5×10^6 cells/mL and stained using a LIVE/DEAD™ Fixable Blue Cell Dead Stain Kit (Molecular Probes™) prior to sorting, according to the manufacturer's protocol. Cell sorting was performed on a BDFACSAria II Cell Sorter (Beckton Dickinson) by first selecting for viable cells emitting low fluorescence under UV excitation, prior to gating under green and red channels to separate GFP+/tdTomato+ and GFP−/tdTomato+ populations. Collected cells were immediately transferred to TRIzol (Invitrogen) after sorting for RNA extraction.

Luciferase assay

Firefly

Assay of Lv.Col2-GFP/fLuc and Lv.CMV-GFP/fLuc transduced monolayer cultures was performed on a Zylux tube luminometer using the Luciferase Assay System (Promega).

Metridia

Secreted luciferase from conditioned media supernatants of Lv.Col2mLuc/EF1-GFP- and Lv.CMVmLuc/EF1-GFP-transduced cultures was assayed using the Ready-To-Glow™ Luciferase Reporter Assay (Takara Bio).

RT-PCR

To measure relative mRNA levels, total RNA was extracted from either pooled aggregates (*n* = 5) and hydrogels (*n* = 2) after 21 d of chondrogenic induction or sorted cell populations, by phenol:chloroform

Table 2. Primers sequences for RT-qPCR. F: forward primer; R: reverse primer.

Gene	Sequence	Species
COL2A1	F: 5'-CTGGTCTCAAAGGCGAACAAG-3'	Equine
	R: 5'-GCACCTCTTTTGCCTTCTTCAC-3'	
SOX9	F: 5'-CAGGTGCTCAAGGGCTACGA-3'	
	R: 5'-GACGTGAGGCTTGTTCTTGCT-3'	
RPLPO	F: 5'-CTGATTACACCTTCCCACTTGCT-3'	
	R: 5'-AGCCACAAATGCAGATGGATCA-3'	
18S	F: 5'-CGGCTTTGGTGACTCTAGATAACC-3'	
	R: 5'-CCATGGTAGGCACAGCGACTA-3'	
GFP	F: 5'-GTGGACAGCCACATGCACTT-3'	Copepod
	R: 5'- GTGCTGGTACTCCACGATGC-3'	

extraction using TRIzol reagent and isopropanol precipitation. cDNA was synthesised from 1 μg of total RNA using the High Capacity RNA-to-cDNA kit (Applied Biosystems) and random hexamer primers, according to the manufacturer's instructions. Real-Time PCR amplification of diluted cDNA products was performed on an Eppendorf Realplex Mastercycler using PerFecta SYBR Green MasterMix (QuantaBio, Beverly, MA, USA) and primers designed from equine gene sequences (Table 2). Relative gene expression was determined from C_t values by normalising to the housekeeping gene, 18S, using the $2^{-\Delta\Delta Ct}$ method (Livak and Schmittgen, 2001).

Confocal imaging

Single photon

Cellular aggregates and PEG hydrogels were fixed in 4 % paraformaldehyde for 30 min at room temperature, washed 3 times in PBS and mounted in Vectashield (Vector Labs). Samples were imaged using a Leica TCS-SP5 (Leica) equipped with a motorised inverted DM IRE2 microscope (Leica). Serial optical sections (1024 × 1024 pixels) were taken at 4 μm intervals using a 20× objective. For aggregates, specimens were imaged using a previously established protocol for intact tissues (Martin-Pena *et al.*, 2006), covering a total volume of 150 × 150 × 150 μm. For PEG-HA hydrogels, the same volume was scanned in multiple locations within the three-dimensional (3D) construct and regions of interest were randomly selected within each location. Individual channels were set for imaging GFP and tdTomato fluorescence signals. For each channel, confocal settings were maintained throughout the samples to allow comparison.

Multi-photon

For full depth, spatial assessment of chondrogenic cells at high resolution, day 21 aggregates were imaged using a Nikon A1RMPsi-STORM 4.0 multi-photon, super resolution imaging system (Nikon Instruments). Aggregates were cut in half and scanned using a 20× objective using a mosaic of 3 by 3 images (1024 × 1024 pixels each) with 10 % overlap in

each z-plane, with each z-plane interspaced by 4 μm and covering a total volume of 1500 × 1500 × 1500 μm.

Analysis

Images were processed using ImageJ software (NIH). Chondrogenic cell distribution in aggregates was determined using maximal z-stack projections and the line profile tool to measure pixel intensity *vs.* depth in the red and green channels. Values were plotted as normalised green:red signal intensity *vs.* depth. Cell counting in PEG-HA hydrogels was performed using the ImageJ cell count plug-in to determine total cell number and mean fluorescence values in red and green channels.

Histology

Aggregates and hydrogels were fixed in 10 % NBF for 30 min at room temperature and embedded in 0.7 % agarose for ease of handling. After dehydration in graded alcohols, the samples were paraffin-embedded and sectioned to 5 μm thickness. Sections representing the centre of each sample were stained using 1 % toluidine blue (Sigma-Aldrich) for the detection of matrix proteoglycan.

Statistical analysis

Quantitative results were shown as representative measurements of a single donor or mean ± standard deviation of biological replicates or multiple donors ($n = 3$). Statistical significance was determined by two-tailed unpaired *t*-test (Fig. 1 and Fig. 5) or two-way ANOVA and subsequent Bonferroni *post-hoc* test (Fig. 4) using GraphPad Prism 5.0. For all tests, $p < 0.05$ was considered statistically significant.

Results

Chondrocyte specific activity of a modified Col2 promoter in primary equine cells

To investigate the activity of the Col2 promoter in equine cells, a bicistronic lentiviral vector (Lv.Col2-GFP/fLuc) was generated, containing the promoter driving co-expression of copepod GFP and firefly
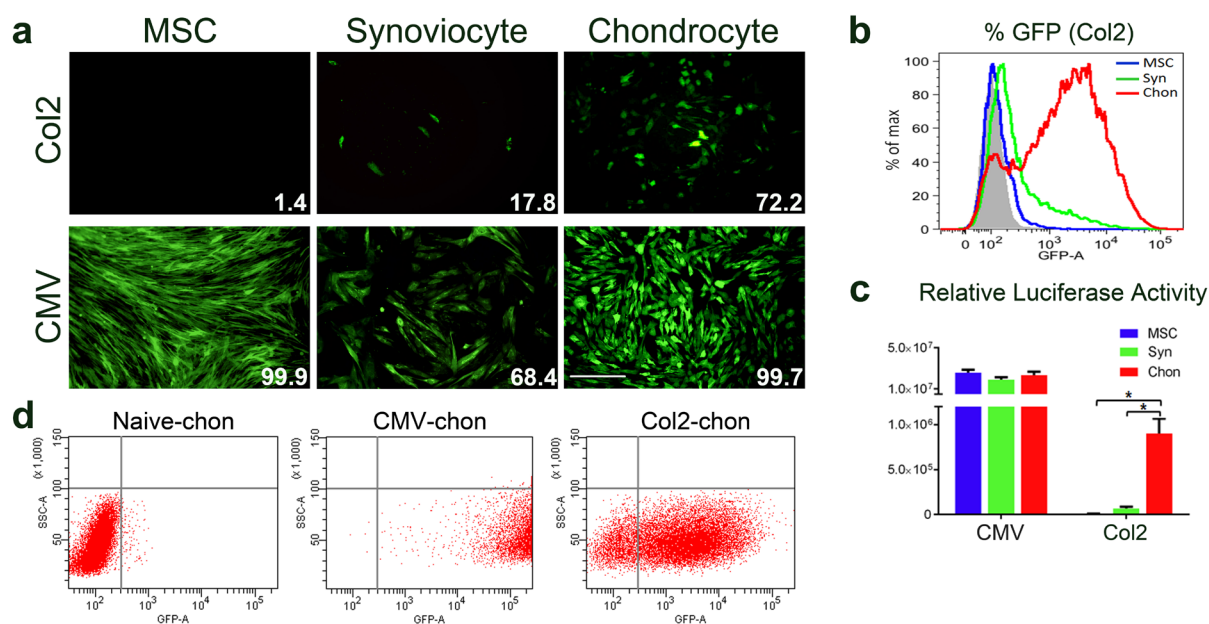
Fig. 1. A modified Col2 promoter exhibited chondrocyte-specific activity in primary equine cells. (a) Green fluorescence images of equine monolayer cultures infected with Lv.Col2-GFP/fLuc (Col2) or Lv.CMV-GFP/fLuc (CMV). Numbers indicate percentage of GFP+ cells as measured by flow cytometry. Scale bar: 250 μm. (**b**) Histogram flow cytometry plot showing the proportion of GFP+ cells after Lv.Col2-GFP/fLuc transduction (grey: naïve cell control). (**c**) Relative luciferase activity among same cell populations. (**d**) Scatter flow cytometry plots showing cell-to-cell variations in GFP fluorescence in Lv-infected chondrocytes. All analyses were performed 72 h after viral transduction. * *p* < 0.05 *vs.* synoviocytes and MSC.

luciferase and responding to chondrogenic induction of human MSCs (Porter *et al.*, 2012). Monolayer cultures of equine MSCs, synovial fibroblasts and chondrocytes were infected and Col2 reporter activity was compared to a control lentiviral construct where GFP is driven by a constitutive CMV promoter (Lv.CMV-GFP/fLuc) (Fig. 1). As expected, CMV-mediated expression of GFP was high in all cultures: analysis of fluorescence by flow cytometry showed that ~ 68-100 % of the cells were positive (Fig. 1**a**,**b**). In contrast, Col2-mediated GFP expression was present in 72 % of primary chondrocytes and ~ 18 % of synoviocytes but absent in undifferentiated MSCs (Fig. 1**a**,**b**). Assay of firefly luciferase in cell lysates revealed the same trend, with chondrocytes exhibiting significantly higher activity (> 10-fold) than synoviocytes and MSCs (* *p* < 0.001; Fig. 1**c**). Cell-to-cell variations within the Col2-GFP+ population were also detected by flow cytometry (scatter plot; Fig. 1**d**). While Lv.CMV-GFP/fLuc-transduced chondrocytes were highly positive for GFP with relatively small variation in fluorescence intensity (middle panel; Fig. 1**d**), Lv.Col2-GFP/fLuc-transduced cultures contained both a negative population and a GFP fluorescence that varied over 2 orders of magnitude (right panel; Fig. 1**d**). Given the relative uniformity of transduction indicated by Lv.CMV-GFP/fLuc, it was concluded that heterogeneity within the Col2-GFP+ population was attributable to cells with varying chondrogenic activities. Based on these findings, Col2-driven

reporter activity was further explored as a sensitive readout for chondrogenesis in 3D culture of primary equine cell populations.

Dual fluorescence reporting revealed heterogeneity within differentiating MSC aggregates
To assess the degree of uniformity of chondrogenesis and visualise temporal, cell-to-cell variations in chondrogenic activity within an MSC population, a dual-fluorescence reporter, Lv.CMV-tom/Col2-GFP, was generated. This reporter vector contained independent expression cassettes under separate regulation of CMV (tdTomato) and modified Col2 (GFP) promoters, enabling the identification of chondrogenic and non-chondrogenic cells within differentiating cell populations. BM-MSCs were transduced with the vector, seeded in aggregate cultures and analysed by confocal microscopy for red and green fluorescence following TGF-β3 stimulation at day 7, 14 and 21 (Fig. 2**a**, upper panels). Z-stack projections of intact aggregates by single photon microscopy revealed abundant tdTomato (red) fluorescence at all time points, indicating high expression of the constitutive CMV-driven reporter. Col2-promoter activation, indicated by either green or a merging of green and red fluorescence (orange), was evident in both unstimulated and day-7-stimulated cultures and identified isolated chondrogenic cells sparsely populated throughout the aggregate. At day 14 and 21, GFP expression markedly increased

with culture duration, but distinct regions of red fluorescence were still visible, indicating the persistence of non-chondrogenic cells. Supporting these findings, toluidine blue metachromasia increased with culture duration in response to TGF-β3 treatment (Fig. 2**a**, lower panels), reflecting ECM accumulation. However, even at 3 weeks, staining was negligible in some areas, consistent with little or no cellular differentiation. Together, these observations revealed striking variations of cellular-level chondrogenic activity within an MSC population in 3D aggregate culture.

To confirm enhanced chondrogenic activity of GFP-expressing cells in differentiating aggregates, cells were isolated by enzymatic digestion after 14 d in culture, separated into tdTomato+/GFP− and
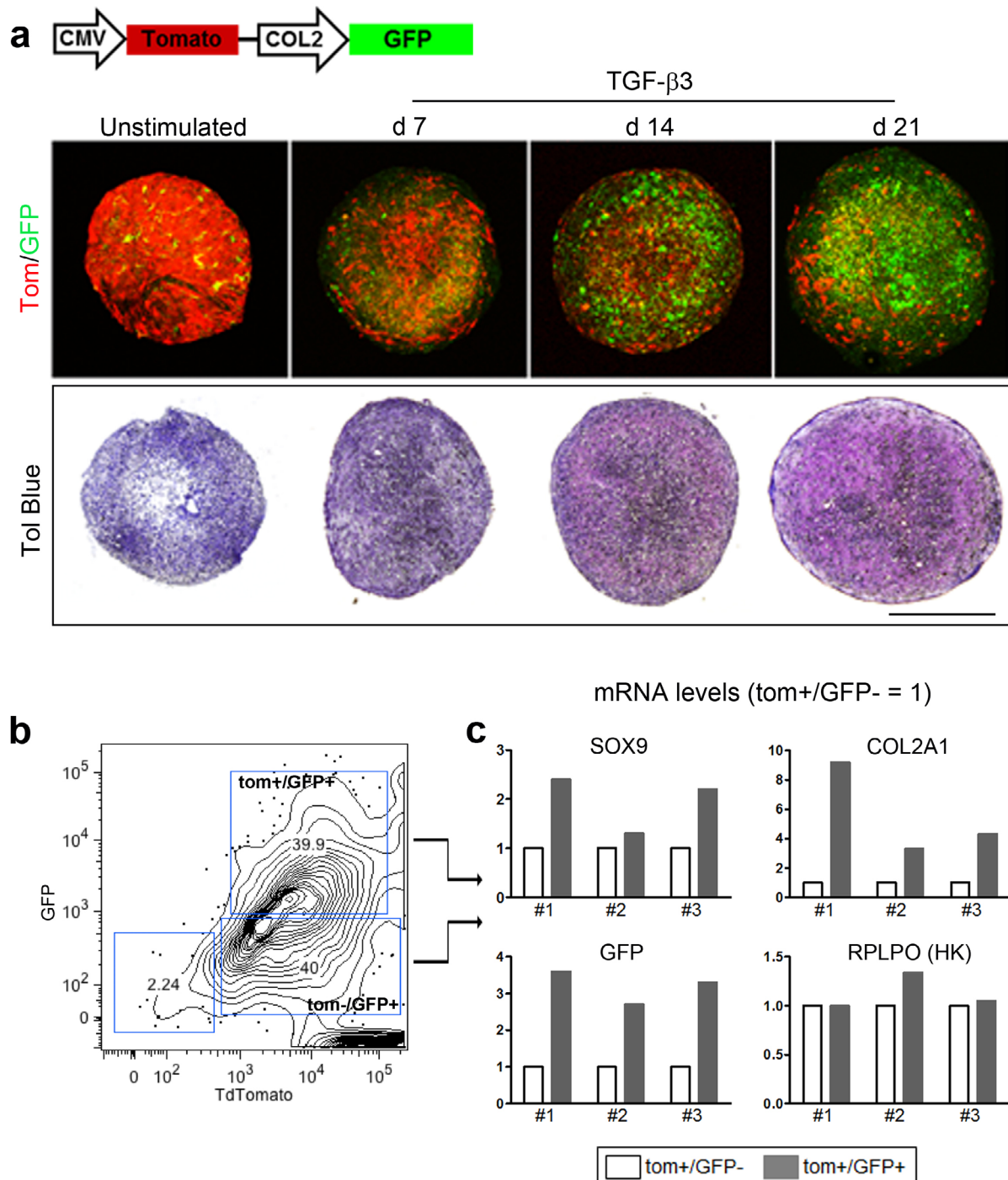

Fig. 2. Identification of chondrogenic cells in differentiating aggregate cultures of MSCs. (**a**) Upper panels: red/green fluorescence images of intact aggregates of BM-MSCs from a 9-year-old donor, modified with a dual fluorescence lentiviral reporter, Lv.CMV-tom/Col2-GFP. Lower panels: toluidine blue staining of aggregate sections at corresponding time points. (**b**) Representative flow cytometry contour plot showing the frequency of fluorescent cell populations in differentiating aggregates isolated at day 14. (**c**) Relative mRNA levels in sorted cell populations (from **b**) deriving from pooled aggregates of 3 separate equine donors, 2 (#1), 9 (#2) and 12 (#3) years old. Scale bar: 500 μm.

tdTomato+/GFP+ cell populations by FACS and analysed for expression of chondrogenic mRNAs (contour plot, Fig. 2**b**). Figure 2**c** shows expression levels in pooled aggregates of 3 separate MSC donors, indicating upregulation of *SOX9* (1.3-2.4-fold) and *COL2A1* (3.3-9.2-fold) in the tdTomato+/GFP+ fraction relative to the tdTomato+/GFP− fraction. GFP mRNA levels, included as a cell sort control, were also elevated (~ 3-fold), while the levels of the non-chondrogenic housekeeping gene, ribosomal protein lateral stalk subunit P0 (RPLP0), did not change between the cell populations.

Spatial variations in chondrogenic activity were further assessed by high-resolution (2-photon) imaging of 21 d aggregates of TGF-β3-treated BM-MSCs (Fig. 3). Aggregates were halved and imaged through the centre to obtain red (tdTomato) and green (GFP) image stacks that were analysed separately to determine fluorescence signal *vs.* depth (Fig. 3**a**). Line plot analysis showing fluorescence intensity profiles (along the x axis) was performed at varying y-plane depths (plots i-v, Fig. 3**b**). Fluorescence ratios > 2 were marked green, denoting high chondrogenic activity, while ratios < 2 were marked red, denoting lower/absent activity. Analysis revealed that highly chondrogenic cells were non-uniformly distributed,

with most of the chondrogenic peaks located (~ 50-400 μm) beneath the aggregate surface (in both x and y planes). This was most evident in plots i and v (y-plane depth ≤ 400 μm) and plots ii and iv (x-plane depth 0-250 μm). Areas of low chondrogenic activity (red) were also concentrated in the deepest regions of the aggregate, represented in plots ii-iv, ~ 300-900 μm, although some chondrogenic cells were still present. These regional variations likely reflected the combined effects of oxygen, nutrient and TGF-β3 gradients on chondrogenic differentiation within the 3D microenvironment.

A secretable luciferase reporter revealed marked variations in chondrogenic potential among MSC populations

For luminescence-based determination of chondrocyte differentiation, a lentiviral construct containing the same modified Col2 promoter driving the expression of secreted *Metridia* luciferase (mLUC) and a constitutive EF1α promoter driving GFP expression for normalisation of transduction efficiency were generated. Through luciferase assay of the conditioned media at various time points, it was assumed that Col2-Luc-reporter-labelled cells would enable longitudinal, non-invasive assessments
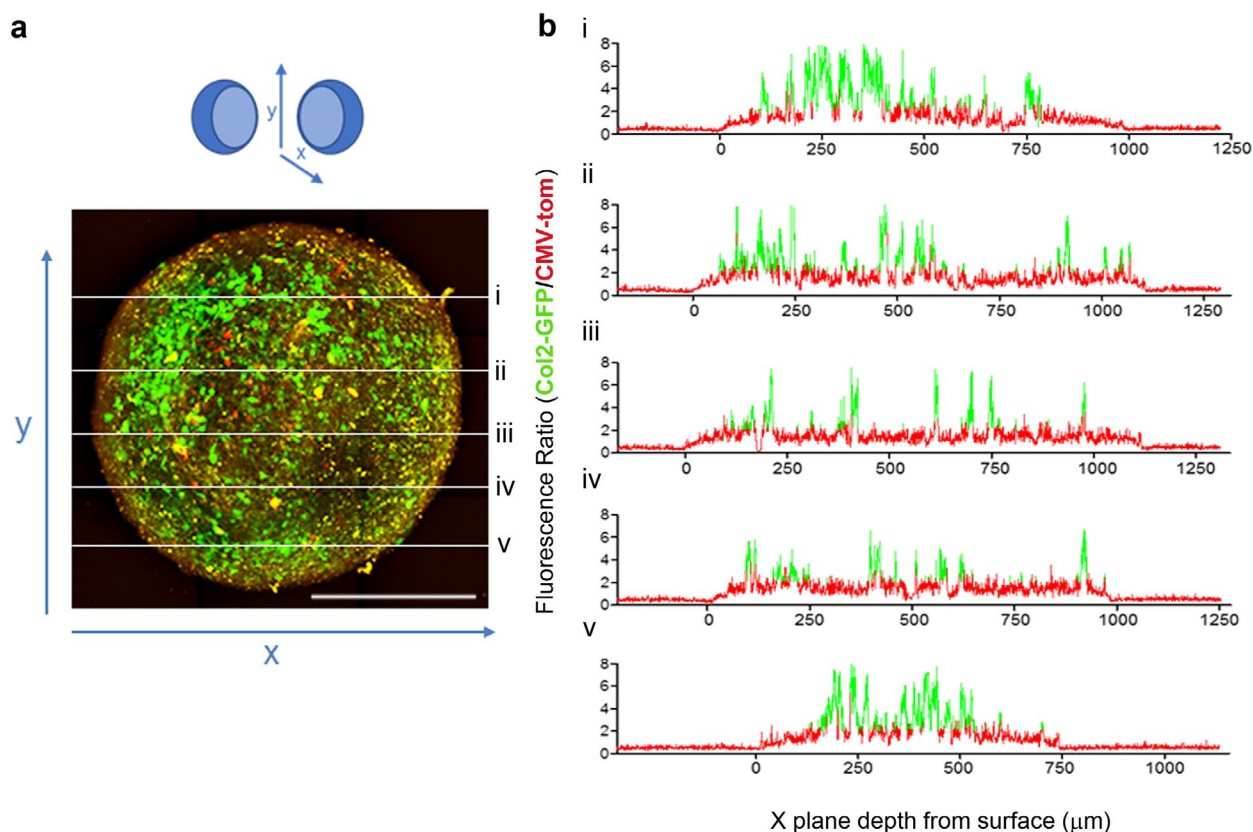

Fig. 3. Regional heterogeneity of chondrogenic cells in differentiating MSC aggregates. (**a**) Merged z-stack projection showing red/green fluorescence, captured by multi-photon imaging of MSC aggregates labelled with Lv.CMV-tom/Col2-GFP and treated with TGF-β3 until day 21. Aggregates were cut in half and imaged through the centre (z-plane depth = 1500 μm). Scale bar: 500 μm. (**b**) Line plots, i-v, showing fluorescent pixel intensity *vs.* depth analysed using ImageJ software. Fluorescence ratios > 2 are marked in green denoting high relative chondrogenic activity, while ratios < 2 are marked in red denoting low/absent activity. Analyses are representative of 4 BM-MSC aggregates.

of differentiation in 3D culture systems that were predictive of overall chondrogenesis, determined by conventional endpoint assays.

Using cells obtained from the same equine donor, chondrogenic activities were compared among MSCs derived from bone marrow (BM), synovium (S) and adipose (A) tissues. MSCs were transduced with Lv.Col2-mLuc/EF1-GFP and grown in aggregate cultures and photopolymerisable PEG-HA hydrogels (Fig. 4a), which are transplantable scaffolds compatible with cell-based cartilage repair (Sharma *et al.*, 2007). To facilitate direct comparisons among cell types, activity was normalised to Lv.CMV-mLuc/EF1-GFP-modified aggregates, cultured in parallel (Fig. 4a). Articular chondrocytes, also harvested from the same donor, were included as a reference for chondrogenic activity. Among MSC types, the luciferase profiles revealed a common trend in both aggregate and hydrogel cultures, with highest chondrogenic activity in BM-MSCs, followed by S-MSCs and A-MSCs at all time points (Fig. 4b,c). Differences among cell types were significant at day 21 in aggregate culture, with A-MSCs exhibiting lower activity as compared to other cells ($p < 0.05$, Fig. 4b), and at day 14 and 21 in PEG-HA cultures, where

BM-MSCs had higher activity than all other cell types ($p < 0.05$, Fig. 4c). Somewhat surprisingly, activity in BM-MSCs was also higher than chondrocytes in aggregate cultures at day 14 and 21 and at all time points in PEG-HA cultures. The luciferase profiles were mostly consistent with the mRNA levels of the chondrogenic markers *SOX9* and *COL2A1* at the endpoint (day 21), indicating the same trend among MSC types (Fig. 4d,e). Similarly, toluidine blue staining intensities of cultures harvested at the endpoint reflected the superior chondrogenesis of BM-MSCs followed by S-MSCs and A-MSCs in both culture systems, in agreement with the luciferase data (Fig. 4f,g). The endpoint analysis also revealed similar chondrogenesis of BM-MSCs relative to chondrocytes in aggregates, also consistent with the luciferase reporter profile (Fig. 4b,d,f). In contrast, chondrocytes in PEG-HA hydrogels had roughly equivalent matrix staining and > 2-fold higher levels of COL2A1 as compared to BM-MSCs, despite exhibiting lower luciferase activity. This discordance could potentially reflect differences in innate stabilities between chondrocyte and MSC phenotypes that were not detectable at the level of Col2 reporter activity.
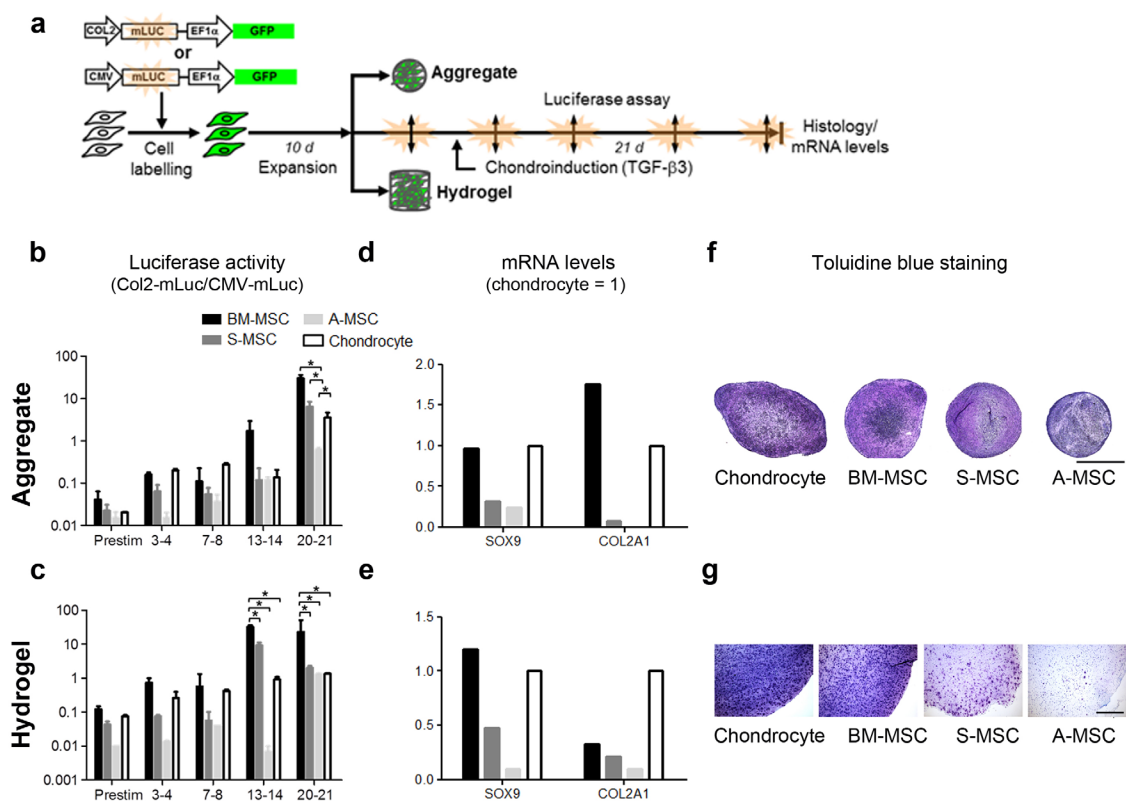

Fig. 4. Luciferase-based, real-time monitoring of chondrogenesis in equine cell populations cultured in aggregates and PEG-HA hydrogels. (**a**) Strategy for cell labelling, culture and analysis. Cells were harvested from a single equine donor (female, 2 years). (**b,c**) Secreted *Metridia* luciferase levels in the conditioned medium 24 h accumulation of TGF-β3-treated aggregate and hydrogel cultures shown as a ratio of Col2-mLuc/CMV-mLuc. Prestimulated controls (Prestim) represent luciferase levels in cultures without TGF-β3 treatment (day 3-4). (**d,e**) Relative mRNA levels of pooled aggregates (5) and hydrogels (2) for each cell type at day 21 endpoint. (**f,g**) Toluidine blue staining of Lv-transduced aggregates and PEG-HA cultures at day 21. * $p < 0.05$. Scale bars: 500 μm.
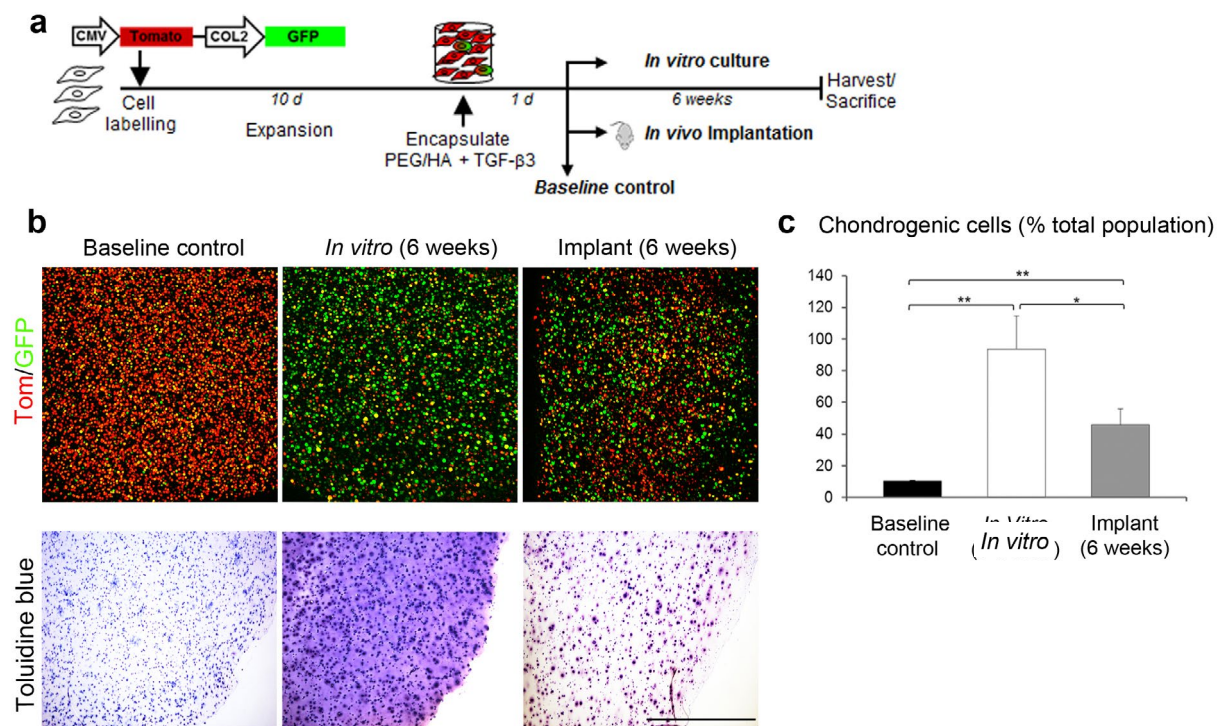
Fig. 5. Comparison of chondrogenic cell fates in PEG-HA hydrogels *in vitro* and *in vivo* using the dual fluorescence reporter, Lv.CMV-tom/Col2-GFP. (a) Strategy for cell labelling, encapsulation and *in vitro* culture/implantation. (**b**) Upper panels: red/green fluorescence images of Lv.CMV-tom/Col2-GFP-transduced chondrocytes in PEG-HA hydrogels. Lower panels: toluidine blue staining of hydrogel sections at corresponding time points. (**c**) Cell counts performed by separate analyses of red and green channels from captured confocal images using ImageJ to determine the relative proportion of chondrogenic (Col2-GFP+) cells within the total cell population (CMV-tdTomato+). Values represent mean of 3 cultures/implants for each group. * $p < 0.05$; ** $p < 0.005$. Scale bar: 500 μm.

Dual fluorescence reporting enabled long-term monitoring of chondrogenic cell fates in PEG-HA implants

To investigate the utility of using fluorescent reporter constructs to determine chondrogenic cell fates *in vivo*, a subcutaneous implantation model was used to track the phenotype of chondrocytes seeded onto PEG-HA scaffolds. Chondrocytes were labelled with Lv.CMV-tom/Col2-GFP, expanded in monolayer and seeded on to PEG-HA hydrogels encapsulated with 100 ng of TGF-β3. After 24 h, the cell-loaded hydrogels were either harvested for analysis (baseline control group), cultured *in vitro* with continuous exposure to chondrogenic induction medium (*in vitro* group) or implanted subcutaneously in athymic mice (implant group) (Fig. 5**a**). Fluorescence image analysis of recovered hydrogels revealed that over 90 % of the total cell population was positive for GFP following *in vitro* differentiation for 6 weeks, increasing from 10 % in the baseline group (*p* < 0.005; Fig. 5**b** upper panels and **c**). This likely reflected re-differentiation of the chondrocyte's phenotype after monolayer expansion through prolonged culture in a 3D microenvironment with continuous exposure to TGF-β3. After 6 weeks *in vivo*, ~ 45 % of the total cell population was GFP+, indicating that initial encapsulation with TGF-β3 could partially restore

the chondrocyte phenotype, but to a lesser degree than under controlled *in vitro* conditions (Fig. 5**c**, *p* < 0.05). In support of these findings, toluidine blue metachromasia indicated greater cellular differentiation under *in vitro* conditions, with intense staining in both peri- and extracellular regions (Fig. 5**b** lower panels). In contrast, recovered implants had less staining, which appeared to be restricted to pericellular regions, while in the baseline group, no significant metachromasia was present. Taken together, these findings indicated that lentiviral-based fluorescent reporters could be used to quantify chondrogenic cell populations in 3D scaffolds and evaluate cellular-level chondrogenesis, providing a platform to compare chondrogenic potencies among chondrocytes and progenitor cell populations in established *in vitro* and *in vivo* models.

Discussion

The presented results demonstrated the use of lentiviral reporter vectors as tools for quantification and spatial assessment of chondrogenesis in primary adult equine cell populations in 3D culture systems. Lentiviral vectors encoding either GFP or luciferase

reporters under conditional activation of a modified Col2 promoter exhibited stable, chondrocyte-specific reporter activity in primary equine chondrocytes and MSCs undergoing TGF-β3-induced chondrogenesis, correlating with histology and mRNA expression levels of *COL2A1* and *SOX9*. Using dual reporter vectors that provided readouts of chondrogenic (Col2) and constitutive (CMV/EF1α) activity, it was possible to (i) discriminate chondrogenic *vs.* non-differentiated cells in aggregate and PEG hydrogel culture systems, (ii) directly compare chondrogenic activities among primary cell populations and (iii) monitor chondrogenic cell fate in hydrogels following subcutaneous implantation *in vivo*.

For *in vitro* monitoring of chondrogenesis, the use of recombinant lentiviral reporter vectors offers several advantages for screening chondrogenic activity of primary cells. They provide stable transgene expression, enabling long-term monitoring of cell fate, and high transduction efficiency (Zhang *et al.*, 2002), reducing the need for additional *ex vivo* manipulations, such as cell sorting or antibiotic selection, that can potentially affect cell differentiation (Cohen *et al.,* 2006; Connell *et al.*, 2016). Transducing titers can be generated with large insert sizes (up to ~ 18 kbp) (Kumar *et al.*, 2001), which allows for the inclusion of multiple reporter genes within single or multiple expression cassettes, enabling several cellular readouts from a single infection.

Using a dual fluorescence reporter vector, Lv.CMV-tom/Col2-GFP, the number of chondrogenic cells (tdTomato+/GFP+) increased in parallel with the level of toluidine blue staining over time in aggregate cultures of MSCs. Notably, despite continued exposure to TGF-β3, large numbers of non-chondrogenic, tdTomato+/GFP− cells were visible at the endpoint (day 21), indicating that a significant population of MSCs exhibited poor or no differentiation within the culture system. This was consistent with the flow cytometric analysis after day 14, where approximately 50 % of the total cell population was GFP+/tdTomato+. Although the persistence of non-differentiated cells within pellet cultures of MSCs is first reported in 1998 (Yoo *et al.*, 1998), the proportion of chondrogenic cells and degree of uniformity within cultures are rarely considered. A non-uniform distribution of differentiating cells was found within TGF-β3-stimulated cultures, with most of the highly chondrogenic cells located proximal (~ 400 μm) to, but not along, the aggregate edge. This may reflect an optimal oxygen level just beneath the pellet surface, as hypoxia (*i.e.* 2-5 % oxygen) increases bone marrow MSC chondrogenesis in pellet culture (Anderson *et al.*, 2016; Boyette *et al.*, 2014). Anderson *et al.* (2016) observe that the MSC response to hypoxia is enhanced in relatively chondrogenic donor preparations. In the present study, fewer cells with high chondrogenic activity were detected within the central regions, which may reflect impaired cellular function resulting from diffusion limitations within the densely packed aggregates. Indeed, tumour

spheroids (> 500 μm) are frequently characterised by proliferation gradients, hypoxic regions and reduced cell viability leading to the formation of necrotic cores (Hirschhaeuser *et al.*, 2010; Laurent *et al.,* 2013; Zanoni *et al.*, 2016). Thus, size and geometric constraints associated with aggregate (sphere)-based culture may mask the true chondrogenic potential of a cell population or chondrogenic factor and should be taken into consideration when performing a screening assay.

For direct, real-time comparisons of chondrogenic activity among cell populations and 3D culture systems, a Col2-driven secretable luciferase reporter was used to reveal greater TGF-β3-mediated chondrogenesis of BM-MSCs relative to S-MSCs and A-MSCs in both aggregate and PEG-hydrogel culture models. Moreover, relative luciferase activity between the cell types remained constant over the differentiation time course and correlated with histologic and mRNA expression levels at the endpoint. Thus, secretable Col2-Luc reporter activity may serve as a potency marker that can predict chondrogenic differentiation of MSCs, providing the opportunity for modification of culturing protocols in real-time, to facilitate the generation of stable, functional cartilage by a particular cell type. This would be of particular benefit to tissue engineering manufacturing processes, which are currently constrained by long-term culturing protocols that rely on endpoint assessments of the final product (Roh *et al.*, 2016).

While interpretation of the study's findings was limited to TGF-β3-driven chondrogenesis from a single equine donor, the superiority of BM-MSCs over A-MSCs is also reported by others (Danisovic *et al.*, 2009; Kohli *et al.*, 2015; Vidal *et al.*, 2008). However, contrary to our observations in equine cells, comparative studies demonstrate enhanced chondrogenesis of S-MSCs relative to BM-MSCs in humans (Shirasawa *et al.*, 2006; Yoshimura *et al.*, 2007) and rats (Sakaguchi *et al.*, 2005). These differences may be attributable to variations of MSC phenotype among species or the use of different growth factor combinations for chondro-induction between studies. Intriguingly, among two very different 3D culture formats – high density aggregates or PEG-HA suspension culture – the relative chondrogenic potentials among BM-, S- and A-MSCs did not change, suggesting that cell-cell adhesion and cell-HA interactions were not critical factors in determining the overall chondrogenic response of the cells to TGF-β3 induction, in the absence of mechanical co-stimulation. However, for optimal chondrogenesis of each MSC type in both culture systems, it will be necessary to perform a broader investigation that incorporates other TGF-β superfamily members, such as BMP-6 (Estes *et al.*, 2006; Hennig *et al.*, 2007) and BMP-7 (Kurth *et al.*, 2007; Miyamoto *et al.*, 2007; Shintani and Hunziker, 2007), which enhance chondrogenic differentiation of A-MSCs and S-MSCs, respectively.

With the long-term goal of application in cartilage defects, the feasibility of using fluorescent reporters to monitor cellular-level chondrogenic cell fates *in vivo* by tracking Lv.CMV-tom/Col2-GFP-labelled chondrocytes in subcutaneously implanted PEG-HA hydrogels was tested. After 6 weeks *in vivo*, almost 50 % of the cell population was chondrogenic (GFP+), significantly more than in monolayer-expanded cultures, but less as compared to PEG-HA hydrogels cultured *in vitro*. This was not surprising as *in vivo* implants received only a single 100 ng bolus of TGF-β3 during encapsulation, while TGF-β3 stimulation *in vitro* was continuous, with repeated growth factor addition every 4 d. Indeed, a single TGF-β3 dose was also not sufficient for reproducible equine MSC differentiation in the same study (data not shown), reflecting the need for sustained growth factor delivery systems to promote cellular differentiation or long-term maintenance of the chondrocyte phenotype *in vivo* (Lam *et al.*, 2015; Rey-Rico and Cucchiarini, 2017).

Conclusions

Variations associated with MSC isolation and culture, as well as poor characterisation of primary cell populations, have greatly impeded the clinical translation of MSCs in cartilage-repair applications (Tanavde *et al.*, 2015). In large animal models, such as the horse –an essential preclinical model for orthopaedic conditions (Hurtig *et al.*, 2011) – this problem is exacerbated by the lack of equine-specific antibodies, as well as the relatively small number of equine-specific gene and protein markers. In the present study, using equine cells as a test system, the utility of using transgenic lentiviral-based reporter vectors as tools for objective assessment of chondrogenesis in preclinical cell-based repair studies was demonstrated. The implementation of these reporters across laboratories will advance the development of standardised protocols and help promoting consensus among investigators with regard to cell types, scaffolds and chondro-induction methods for clinical translation of cell-based therapies for cartilage repair.

Acknowledgements

References

Anderson DE, Markway BD, Bond D, McCarthy HE, Johnstone B (2016) Responses to altered oxygen tension are distinct between human stem cells of high and low chondrogenic capacity. Stem Cell Res Ther **7**: 154.

Bornes TD, Adesida AB, Jomha NM (2014) Mesenchymal stem cells in the treatment of traumatic articular cartilage defects: a comprehensive review. Arthritis Res Ther **16**: 432.

Boyette LB, Creasey OA, Guzik L, Lozito T, Tuan RS (2014) Human bone marrow-derived mesenchymal stem cells display enhanced clonogenicity but impaired differentiation with hypoxic preconditioning. Stem Cells Transl Med **3**: 241-254.

Cohen S, Samadikuchaksaraei A, Polak JM, Bishop AE (2006) Antibiotics reduce the growth rate and differentiation of embryonic stem cell cultures. Tissue Eng **12**: 2025-2030.

Connell JP, Augustini E, Cheng S, Benavides OM, Ruano R, Jacot JG (2016) Effect of passage, sorting, and media on differentiation capacity and marker expression in amniotic fluid stem cells. Cel Mol Bioeng **9**: 139-150.

Danisovic L, Varga I, Polak S, Ulicna M, Hlavackova L, Bohmer D, Vojtassak J (2009) Comparison of *in vitro* chondrogenic potential of human mesenchymal stem cells derived from bone marrow and adipose tissue. Gen Physiol Biophys **28**: 56-62.

Dull T, Zufferey R, Kelly M, Mandell RJ, Nguyen M, Trono D, Naldini L (1998) A third-generation lentivirus vector with a conditional packaging system. J Virol **72**: 8463-8471.

Estes BT, Wu AW, Guilak F (2006) Potent induction of chondrocytic differentiation of human adipose-derived adult stem cells by bone morphogenetic protein 6. Arthritis Rheum **54**: 1222-1232.

Goldberg A, Mitchell K, Soans J, Kim L, Zaidi R (2017) The use of mesenchymal stem cells for cartilage repair and regeneration: a systematic review. J Orthop Surg Res **12**: 39.

He F, Chen X, Pei M (2009) Reconstruction of an *in vitro* tissue-specific microenvironment to rejuvenate synovium-derived stem cells for cartilage tissue engineering. Tissue Eng Part A **15**: 3809-3821.

Hennig T, Lorenz H, Thiel A, Goetzke K, Dickhut A, Geiger F, Richter W (2007) Reduced chondrogenic potential of adipose tissue derived stromal cells correlates with an altered TGFbeta receptor and BMP profile and is overcome by BMP-6. J Cell Physiol **211**: 682-691.

Hirschhaeuser F, Menne H, Dittfeld C, West J, Mueller-Klieser W, Kunz-Schughart LA (2010) Multicellular tumor spheroids: an underestimated tool is catching up again. J Biotechnol **148**: 3-15.

Huang YZ, Xie HQ, Silini A, Parolini O, Zhang Y, Deng L, Huang YC (2017) Mesenchymal stem/progenitor cells derived from articular cartilage, synovial membrane and synovial fluid for cartilage

regeneration: current status and future perspectives. Stem Cell Rev **13**: 575-586.

Hung CT, Henshaw DR, Wang CC, Mauck RL, Raia F, Palmer G, Chao PH, Mow VC, Ratcliffe A, Valhmu WB (2000) Mitogen-activated protein kinase signaling in bovine articular chondrocytes in response to fluid flow does not require calcium mobilization. J Biomech **33**: 73-80.

Hurtig MB, Buschmann MD, Fortier LA, Hoemann CD, Hunziker EB, Jurvelin JS, Mainil-Varlet P, McIlwraith CW, Sah RL, Whiteside RA (2011) Preclinical studies for cartilage repair: recommendations from the International Cartilage Repair Society. Cartilage **2**: 137-152.

Jayasuriya CT, Chen Q (2015) Potential benefits and limitations of utilizing chondroprogenitors in cell-based cartilage therapy. Connect Tissue Res **56**: 265-271.

Johnstone B, Hering TM, Caplan AI, Goldberg VM, Yoo JU (1998) *In vitro* chondrogenesis of bone marrow-derived mesenchymal progenitor cells. Exp Cell Res **238**: 265-272.

Kan A, Ikeda T, Saito T, Yano F, Fukai A, Hojo H, Ogasowara T, Ogata N, Nakamura K, Chung UI, Kawaguchi H (2009) Screening of chondrogenic factors with a real-time fluorescence-monitoring cell line ATDC5-C2ER: identification of sorting nexin 19 as a novel factor. Arthritis Rheum **60**: 3314-3323.

Khan WS, Adesida AB, Tew SR, Longo UG, Hardingham TE (2012) Fat pad-derived mesenchymal stem cells as a potential source for cell-based adipose tissue repair strategies. Cell Prolif **45**: 111-120.

Kim JH, Lee SR, Li LH, Park HJ, Park JH, Lee KY, Kim MK, Shin BA, Choi SY (2011) High cleavage efficiency of a 2A peptide derived from porcine teschovirus-1 in human cell lines, zebrafish and mice. PLoS One **6**: e18556.

Kohli N, Wright KT, Sammons RL, Jeys L, Snow M, Johnson WE (2015) An *in vitro* comparison of the incorporation, growth, and chondrogenic potential of human bone marrow *versus* adipose tissue mesenchymal stem cells in clinically relevant cell scaffolds used for cartilage repair. Cartilage **6**: 252-263.

Kumar M, Keller B, Makalou N, Sutton RE (2001) Systematic determination of the packaging limit of lentiviral vectors. Hum Gene Ther **12**: 1893-1905.

Kurth T, Hedbom E, Shintani N, Sugimoto M, Chen FH, Haspl M, Martinovic S, Hunziker EB (2007) Chondrogenic potential of human synovial mesenchymal stem cells in alginate. Osteoarthritis Cartilage **15**: 1178-1189.

Lam J, Lu S, Kasper FK, Mikos AG (2015) Strategies for controlled delivery of biologics for cartilage repair. Adv Drug Deliv Rev **84**: 123-134.

Laurent J, Frongia C, Cazales M, Mondesert O, Ducommun B, Lobjois V (2013) Multicellular tumor spheroid models to explore cell cycle checkpoints in 3D. BMC Cancer **13**: 73.

Livak KJ, Schmittgen TD (2001) Analysis of relative gene expression data using real-time quantitative PCR and the 2(-delta delta C(T)) method. Methods **25**: 402-408.

Lo Monaco M, Merckx G, Ratajczak J, Gervois P, Hilkens P, Clegg P, Bronckaers A, Vandeweerd JM, Lambrichts I (2018) Stem cells for cartilage repair: preclinical studies and insights in translational animal models and outcome measures. Stem Cells Int **2018**: 9079538.

Mackay AM, Beck SC, Murphy JM, Barry FP, Chichester CO, Pittenger MF (1998) Chondrogenic differentiation of cultured human mesenchymal stem cells from marrow. Tissue Eng **4**: 415-428.

Martin-Pena A, Acebes A, Rodriguez JR, Sorribes A, de Polavieja GG, Fernandez-Funez P, Ferrus A (2006) Age-independent synaptogenesis by phosphoinositide 3 kinase. J Neurosci **26**: 10199-10208.

Matricali GA, Dereymaeker GP, Luyten FP (2010) Donor site morbidity after articular cartilage repair procedures: a review. Acta Orthop Belg **76**: 669-674.

Matsumoto T, Okabe T, Ikawa T, Lida T, Yasuda H, Nakamura H, Wakitani S (2010) Articular cartilage repair with autologous mesenchymal stem cells. J Cell Physiol **225**: 291-295.

McCarthy HE, Bara JJ, Brakspear K, Singhrao SK, Archer CW (2012) The comparison of equine articular cartilage progenitor cells and bone marrow-derived stromal cells as potential cell sources for cartilage repair in the horse. Vet J **192**: 345-351.

McLeod CM, Mauck RL (2017) On the origin and impact of mesenchymal stem cell heterogeneity: New insights and emerging tools for single cell analysis. Eur Cell Mater **34**: 217-231.

Miyamoto C, Matsumoto T, Sakimura K, Shindo H (2007) Osteogenic protein-1 with transforming growth factor-beta1: potent inducer of chondrogenesis of synovial mesenchymal stem cells *in vitro*. J Orthop Sci **12**: 555-561.

Nathan S, Das De S, Thambyah A, Fen C, Goh J, Lee EH (2003) Cell-based therapy in the repair of osteochondral defects: a novel use for adipose tissue. Tissue Eng **9**: 733-744.

Orth P, Madry H (2015). Complex and elementary histological scoring systems for articular cartilage repair. Histol Histopathol **30**: 911-919.

Outani H, Okada M, Yamashita A, Nakagawa K, Yoshikawa H, Tsumaki N (2013) Direct induction of chondrogenic cells from human dermal fibroblast culture by defined factors. PLoS One **8**: e77365. DOI: 10.1371/journal.pone.0077365.

Padmashali RM, Mistriotis P, Liang MS, Andreadis ST (2014) Lentiviral arrays for live-cell dynamic monitoring of gene and pathway activity during stem cell differentiation. Mol Ther **22**: 1971-1982.

Palmer GD, Chao Ph PH, Raia F, Mauck RL, Valhmu WB, Hung CT (2001) Time-dependent aggrecan gene expression of articular chondrocytes in response to hyperosmotic loading. Osteoarthritis Cartilage **9**: 761-770.

Pei M, Luo J, Chen Q (2008) Enhancing and maintaining chondrogenesis of synovial fibroblasts

by cartilage extracellular matrix protein matrilins. Osteoarthritis Cartilage **16**: 1110-1117.

Porter RM, Liu F, Ferreira E, Lunstord EP, Robichaud K, Evans CH (2012) Characterization of a fluorescence-luminescence reporter construct for extended evaluation of chondrogenesis *in vitro* and *in vivo*. Trans Orthop Res Soc 0559. Provide URL

Rey-Rico A, Cucchiarini M (2017) Smart and controllable rAAV gene delivery carriers in progenitor cells for human musculoskeletal regenerative medicine with a focus on the articular cartilage. Curr Gene Ther **17**: 127-138.

Roelofs AS, Rocke JPJ, DeBari C (2013) Cell-based approaches to joint surface repair: a research perspective. OA and Cart **21**: 892-900.

Roh KH, Nerem RM, Roy K (2016) Biomanufacturing of therapeutic cells: state of the art, current challenges, and future perspectives. Annu Rev Chem Biomol Eng **7**: 455-478.

Sakaguchi Y, Sekiya I, Yagishita K, Muneta T (2005) Comparison of human stem cells derived from various mesenchymal tissues: superiority of synovium as a cell source. Arthritis Rheum **52**: 2521-2529.

Sharma B, Williams CG, Khan M, Manson P, Elisseeff JH (2007) *In vivo* chondrogenesis of mesenchymal stem cells in a photopolymerized hydrogel. Plast Reconstr Surg **119**: 112-120.

Shintani N, Hunziker EB (2007) Chondrogenic differentiation of bovine synovium: bone morphogenetic proteins 2 and 7 and transforming growth factor beta1 induce the formation of different types of cartilaginous tissue. Arthritis Rheum **56**: 1869-1879.

Shirasawa S, Sekiya I, Sakaguchi Y, Yagishita K, Ichinose S, Muneta T (2006) *In vitro* chondrogenesis of human synovium-derived mesenchymal stem cells: optimal condition and comparison with bone marrow-derived cells. J Cell Biochem **97**: 84-97.

Stokes DG, Liu G, Dharmavaram R, Hawkins D, Piera-Velazquez S, Jimenez SA (2001) Regulation of type-II collagen gene expression during human chondrocyte de-differentiation and recovery of chondrocyte-specific phenotype in culture involves Sry-type high-mobility-group box (SOX) transcription factors. Biochem J **360**: 461-470.

Tanavde V, Vaz C, Rao MS, Vemuri MC, Pochampally RR (2015) Research using mesenchymal stem/stromal cells: quality metric towards developing a reference material. Cytotherapy **17**: 1169-1177.

Veronesi F, Maglio M, Tschon M, Aldini NN, Fini M (2013) Adipose-derived mesenchymal stem cells for cartilage tissue engineering: state-of-the-art in *in vivo* studies. J Biomed Mater Res A **102**: 2448-2466

Vidal MA, Robinson SO, Lopez MJ, Paulsen DB, Borkhsenious O, Johnson JR, Moore RM, Gimble JM (2008) Comparison of chondrogenic potential in equine mesenchymal stromal cells derived from adipose tissue and bone marrow. Vet Surg **37**: 713-724.

Watson RS, Broome TA, Levings PP, Rice BL, Kay JD, Smith AD, Gouze E, Gouze JN, Dacanay EA, Hauswirth WW, Nickerson DM, Dark MJ, Colahan PT, Ghivizzani SC (2013) scAAV-mediated gene transfer of interleukin-1-receptor antagonist to synovium and articular cartilage in large mammalian joints. Gene Ther **20**: 670-677.

Wickham MQ, Erickson GR, Gimble JM, Vail TP, Guilak F (2003) Multipotent stromal cells derived from the infrapatellar fat pad of the knee. Clin Orthop Relat Res **412**: 196-212.

Williams R, Khan IM, Richardson K, McCarthy HE, Analbelsi T, Singhrao SK, Dothwaite GP, Jones RE, Baird DM, Lewis H, Roberts S, Shaw HM, Dudhia J, Fairclough J, Briggs T, Archer CW (2010) Identification and clonal characterisation of a progenitor cell sub-population in normal human articular cartilage. PLoS One **5**: e13246.

Yoo JU, Barthel TS, Nishimura K, Solchaga L, Caplan AI, Goldberg VM, Johnstone B (1998) The chondrogenic potential of human bone-marrow-derived mesenchymal progenitor cells. J Bone Joint Surg Am **80**: 1745-1757.

Yoshimura H, Muneta T, Nimura A, Yokoyama A, Koga H, Sekiya I (2007) Comparison of rat mesenchymal stem cells derived from bone marrow, synovium, periosteum, adipose tissue, and muscle. Cell Tissue Res **327**: 449-462.

Zanoni M, Piccinini F, Arienti C, Zamangi A, Santi S, Polico R, Bevilacqua A, Tesei A (2016) 3D tumor spheroid models for *in vitro* therapeutic screening: a systematic approach to enhance the biological relevance of data obtained. Sci Rep **6**: 19103.

Zhang XY, La Russa VF, Bao L, Kolls J, Schwarzenberger P, Reiser J (2002) Lentiviral vectors for sustained transgene expression in human bone marrow-derived stromal cells. Mol Ther **5**: 555-565.

Zhou G, Lefebvre V, Zhang Z, Eberspaecher H, de Crombrugghe B (1998) Three high mobility group-like sequences within a 48-base pairenhancer of the Col2a1 gene are required for cartilage-specificexpression *in vivo*. J Biol Chem **273**: 14989-14997.

Discussion with Reviewers

Marcy Zenoby-Wong: How sorting of the Col2+ cells could be used to advance cartilage therapies?

Authors: Cell sorting offers the possibility of selecting homogenous populations of differentiated (Col2-GFP+/CMV-tdTomato+) from less/non-differentiated (Col2-GFP−/CMV-tdTomato+) MSCs for evaluation in experimental models of cartilage repair. Comparative studies between sorted *versus* unsorted (mixed) populations may help determining the optimal differentiation state of effective MSC-based repair following implantation into cartilage defects. Current strategies in preclinical studies adopt various levels of pre-stimulation of MSCs with chondrogenic factors (Bornes *et al.*, 2014; Goldberg *et al.*, 2017); yet, how this conditioning, as it relates to cellular-level differentiation status, affects cell engraftment,

survival, integration and overall repair within a lesion is not extensively explored.

Marcy Zenoby-Wong: What would be the clinical consequence of using a heterogeneous population of MSCs?

Authors: Cellular heterogeneity is an inherent feature of primary MSC populations and poses a significant hurdle for cartilage regeneration therapies. At present, pre-clinical studies fail to extend beyond proof-of-concept due to a poor characterisation of MSC populations and the lack of standardised methods for quantifying chondrogenic potential (Tanavde *et al.*, 2015). Consequently, repair studies have yet to demonstrate efficacy and the contribution of implanted MSCs to repair tissue is poorly understood. Clinically, heterogeneity in the cellular composition of MSC preparations will lead to inconsistent repair and unacceptably high variability in patient outcome. Efforts to reduce or control cellular heterogeneity, through the development of selection-based tools that enable quantification of proliferative capacity and multipotency, will be needed for reparative strategies involving MSCs for mainstream application.

Chris Evans: Are the authors surprised that 18 % of synoviocytes express GFP from a Col2 promoter? Would it be possible to sort these cells to determine whether they are spontaneously chondrogenic?

Authors: While the synovium is a source of stem cells with chondrogenic potential (Jones and Pai, 2012, additional reference), the study's results inferred that there was a resident cell subpopulation with a chondrocytic phenotype in primary cultures of equine synoviocytes that did not require derivation through cell expansion and stimulation with defined chondro-inductive growth factors. This finding was not a complete surprise as a fate mapping study shows that adult chondrocytes and synovial fibroblasts emerge from a common progenitor during development of synovial joints (Koyama *et al.*, 2008, additional reference). Roelofs *et al.* (2017, additional reference) demonstrate that endogenous populations of growth differentiation factor 5 (GDF5)+ cells

in the joint interzone contribute to both synovial hyperplasia and cartilage repair *in vivo*. Interestingly, in osteoarthritis cartilage, pannus-like soft tissue also contains cells expressing type II collagen and aggrecan, suggesting repair by cells of synovial origin in the early stage disease (Yuan *et al.*, 2004, additional reference). These reports are in line with the present study on osteoarthritis in equine joints where extensive areas of contact between synovium and lesional as well as non-lesional articular cartilage are observed, suggesting direct, physical remodelling of cartilage by synovial tissues. Further investigation will be necessary to determine whether the synovial-derived Col2-GFP cells identified in the present study were spontaneously chondrogenic and served as a potential source for cartilage repair.

Additional References

Jones BA, Pei M (2012) Synovium-derived stem cells: a tissue-specific stem cell for cartilage engineering and regeneration Tissue Eng Part B Rev **18**: 301-311.

Koyama E, Shibukawa Y, Nagayama M, Sugito H, Young B, Yuasa T, Okabe T, Ochiai T, Kamiya N, Rountree RB, Kingsley DM, Iwamoto M, Enomoto-Iwamoto M, Pacifici M (2008) A distinct cohort of progenitor cells participates in synovial joint and articular cartilage formation during mouse limb skeletogenesis. Dev Biol **316**: 62-73.

Roelofs AJ, Zupan J, Riemen AHK, Kania K, Ansboro S, White N, Clark SM, De Bari C (2017) Joint morphogenetic cells in the adult mammalian synovium. Nat Commun **8**: 15040.

Yuan G-H, Tanaka M, Masuko-Hongo K, Shibakawa A, Kato T, Nishioka K, Nakamura H (2004) Characterization of cells from pannus-like tissue over articular cartilage of advanced osteoarthritis. Osteoarthritis Cartilage **12**: 38-45.